

Semi-Supervised Machine Learning Model For Sizing of Distributed Renewable Energy Sources

Kuber Kushwaha*, Graduate Student Member, IEEE and Ch. Venkaiah#, Senior Member, IEEE

Department of Electrical Engineering, National Institute of Technology Warangal, Hanumakonda, TS, India

*kuberkushwaha08@ieee.org, #ch.venkaiah@ieee.org

Abstract—This study presents a significant advancement in energy planning for grid-connected homes with plug-in electric vehicles (PEVs). A cutting-edge model has been developed to accurately size battery storage systems (BSS), small wind turbines (SWT), and solar photovoltaic panels (SPV). The model considers real-world factors like grid limitations and component degradation, resulting in more realistic outcomes. To tackle the complex problem, a semi-supervised machine learning algorithm approach was employed, combining unsupervised and supervised methods. This innovative algorithm outperforms traditional machine learning techniques and metaheuristic methods. By analyzing a wide range of configurations using both labeled and unlabeled data, the optimal setup to minimize electricity costs is identified. In addition, a real-time, rule-based, and efficient home energy management system is presented. The study is based on real data from Australia, including temperature, wind speed, solar radiation, load, and economic and technical information on solar, wind, batteries, and plug-in electric vehicles. The results demonstrate that the proposed model significantly outperforms the conventional Group Method of Data Handling (GMDH), marking a significant advancement in energy planning technology.

Index Terms—Inverters, semi-supervised machine learning, plug-in electric vehicle, DRES, BSS.

NOMENCLATURE

Superscripts

<i>act</i>	Actual
<i>chr</i>	Charging
<i>dch</i>	Discharging
<i>max</i>	Maximum limit
<i>min</i>	Minimum limit
<i>plt</i>	Project lifetime

Subscripts

<i>dpd</i>	Dumped power
<i>drs</i>	Distributed renewable energy sources
<i>exp</i>	Export
<i>hm</i>	Home
<i>hmpev</i>	Total load, home plus pev
<i>imp</i>	Import
<i>inv</i>	Inverters
<i>j</i>	Types of components

Abbreviations

<i>AC</i>	Annual COE exchange between home and grid (\$)
<i>GC</i>	Capital cost for charger of EV (\$)
<i>IOCT</i>	Initial operating cell temperature (°C)
<i>TPC</i>	Total net present cost of components (\$)

Parameters

<i>D</i>	Annual degradation (%)
<i>I_{gs}</i>	Incident global solar radiation
<i>I_S</i>	Standard insolation (kWh/m ²)
<i>K_p</i>	Power temperature coefficient (%/°C)
<i>t</i>	Time (hr)
<i>T_{am}</i>	Ambient temperature (°C)
<i>T_c</i>	Cell temperature (°C)
<i>Y_d</i>	Derating factor resulting from dust accumulation
<i>β</i>	Numbers of optimized components

I. INTRODUCTION

Technological advances bring benefits like improved energy efficiency, safety, and affordability to wind, solar, and battery storage systems (BSS). The growing demand for residential plug-in electric vehicles (PEVs) is significantly driving the necessity for home fast-chargers [1]. The PEV, equipped with a fast charger, provides the convenience of rapid vehicle charging [2]. To achieve an intelligent, cost-effective, and eco-friendly energy supply for PEVs and homes, it is essential to install distributed renewable energy sources (DRESs) and BSSs [3]. Utilizing small wind turbines (SWTs) and rooftop solar photovoltaics (SPVs) is a feasible choice for implementing Distributed Renewable Energy Systems (DRESs) in residential homes. In capacity planning (sizing), energy management systems (EMS), and economic analysis, a grid-connected home featuring a TOU tariff, PEV, DRESs, and BSS poses a complex problem. For such a house, developing an effective EMS is crucial to determine optimal sizes for BSS and DRES at the most cost-effective rates. Incentives for purchasing SPV, SWT, and BSS include time-varying electricity pricing are provided by network operators and government subsidies for SPV and BSS acquisitions. Numerous studies in the residential sector have been conducted to address the sizing challenges associated with renewable sources systems. The optimal capacities for BSS and SPV in a grid-tied house without a PEV were identified in [4]. Capacity planning was explored in [5], but an EMS was not specifically developed for its operation. In [7], a stochastic optimization framework was investigated, considering the influence of real-time pricing (RTP). Since an electric vehicle (EV) is probably being charged at home and will probably need to be charged during peak hours, this is very crucial. But with a BSS, TOU can become more cost-effective. However, the studies conducted so far have not taken into account the impact of PEV with SSML on the optimal capacity planning of the DRES model problem. Several studies

have investigated optimal capacity planning considering PEV. In [10], PEVs were integrated into residential neighborhoods, maximizing the capacity of solar, wind, and battery. Resource organization and distribution of PEV charging stations were studied in [1]. The impact of PEV's load modeling on the planning model was analyzed in [1]. Nevertheless, previous studies have not tackled the sizing aspect for homes connected to the grid with fast-charging PEVs. This remains a significant gap in achieving optimal planning for a renewable energy sources system, and addressing it can lead to effective cost reduction through the adoption of a fast-charging model with SSML approach. Traditional mathematical techniques often face challenges in addressing sizing issues, particularly in dealing with non-linearities and the intricacies of problems such as determining battery lifespan based on degradation [8]. Consequently, metaheuristic techniques like tabu search algorithm (TSA) [9] and particle swarm optimization (PSO) [5] are preferred over conventional methods. Yet, in dealing with vast search spaces, these metaheuristic approaches show shortages like extended computational time and limited exploration efficiency. To overcome these challenges, SSML algorithm, known for its model-free nature and adeptness in handling complex issues, can be employed [1]. Because the fast charger enables rapid PEV charging, it enhances the flexibility in EMS design. However, this study introduces a new, specially designed EMS with unique rules for homes equipped with fast-charging PEVs, aiming to reduce electricity costs. Considering that State of Charge (SOC) fluctuates between 20% and 100%, typical slow chargers, with a rating of approximately 7 kW, can recharge a 100 kWh capacity of PEV in 12 hours. Conversely, fast chargers, specifically designed for residential use, have a 22 kW rating, allowing them to recharge PEVs in fewer than five hours [1]. While the model designed for the purpose is comprehensive, it integrates actual measured data from an Australian case study to yield meaningful results. The model developed encompasses the degradations of battery, solar, and wind-turbine. Investigations were conducted to assess the impacts on optimization outcomes, considering factors such as rapid charger power, maximum import/export powers from/to the grid, and the battery capacity of the PEV.

The key advancements achieved by this study, in comparison to previous studies, can be summarized as follows:

- A novel capacity planning model is developed for BSS, SWT, and SPV in grid-connected houses with fast-charging PEVs. The model integrates realistic parameters, such as grid limitations and actual data, incorporating an offset value and accounting for component degradation.
- A semi-supervised machine learning algorithm, combining both unsupervised and supervised approaches, is employed to address the capacity planning problem. The semi-supervised algorithm shows encouraging results when compared to alternative machine learning (ML) and metaheuristic methods.

The rest of this paper is organized as follows. **Section II** deals with modeling of the system, including the model for the

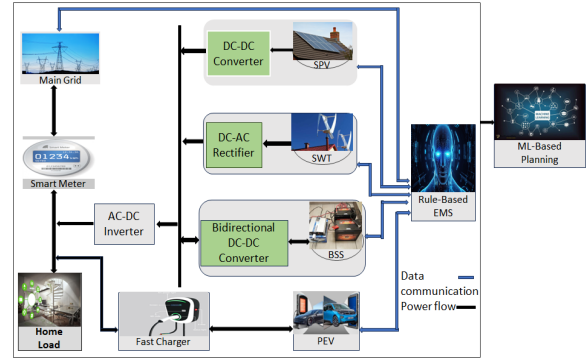


Fig. 1. Overview of the system grid-connected household.

actual DRES, flowchart of the operation strategy, time-of-use tariff model, and inverter model. **Section III** describes the optimal capacity planning model containing problem formulation and constraints, SSML model algorithm. **Section IV** presents the case study. **Section V** presents the results and discussion of this paper. Finally, **Section VI** provides conclusion.

II. MODELLING

In this section, an overview of the work, a flowchart detailing the operation strategy, and the integration of renewable sources model into SSML are presented.

A. Overview of the Present Work

Fig. 1 depicts the configuration of a distributed renewable energy sources system integrated with the main grid, PEV, homes, inverters, choppers, smart meters, fast chargers, and rooftop solar panels, providing an effective and affordable solution for residential areas. The figure also shows the connection of SWT, SPV, and BSS through a DC link bus and converters. This system is planned using Machine Learning algorithm, which avoids charging the BSS from the main grid due to battery degradation. Additionally, the study excludes PEV operations in vehicle-to-grid or vehicle-to-home modes [7].

B. Flowchart of Operation Strategy

This work introduces a novel rule-based home energy management system (HEMS) operation technique for grid-connected houses, providing simplicity, adaptability, and user-friendliness. The real-time strategy, as depicted in Fig.2, factors in time-of-use tariffs, charging rates, electricity costs, time of day, renewable generation, and battery status. It addresses grid restrictions and battery limits, uniquely designed for houses equipped with fast-charging infrastructure.

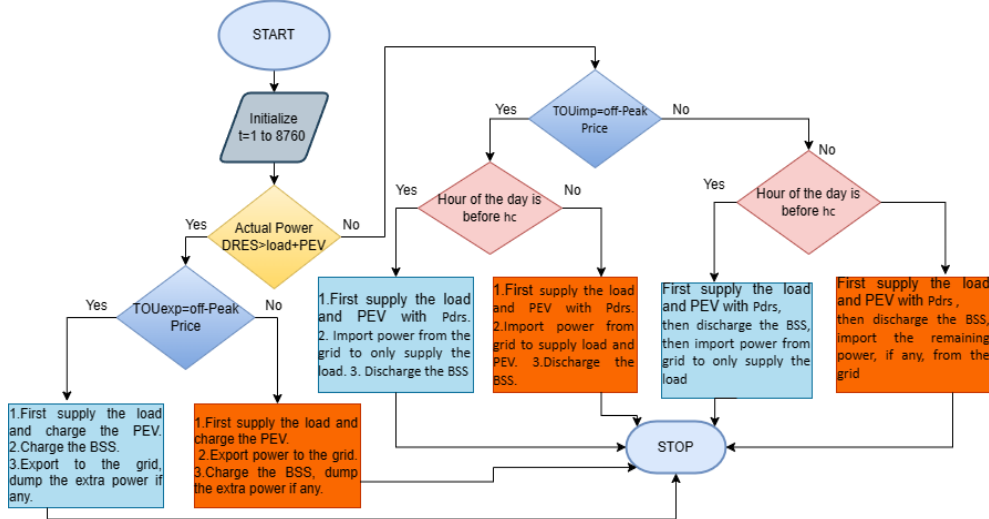


Fig. 2. An HEMS for the proposed model based on real-time rules.

C. Time-of-use (TOU) tariff Model

The TOU tariff technique divides the power price into off-peak (21–07) and peak (08–20) periods, with one-third of the electricity cost charged during off-peak hours [9]. Considering a PEV battery capacity of 100 kWh, a 22 kW fast charger (for household use), and a departure time not earlier than 5 am, the key hour is set at 12 midnight. Even in adverse conditions, with a PEV SOC of 20% and no generation from the battery-solar-wind system, selecting this crucial hour allows the primary 22 kW of grid power to fully charge the PEV in 5 hours (12 midnight to 5 a.m.). The operation strategy recommends identifying a critical hour (hc) to minimize electricity costs. If the PEV arrives before this crucial hour, it incurs charges only for the BSS and DRESSs. Charging the PEV from the main grid is also an option beyond the crucial hour.

D. Mathematical Modelling

1) *DRESSs*: Here, the equation incorporates parameters for SWT and SPV, calculating their output powers from equations (1) and (3), as described in [9] based on real-time data of solar radiation, wind speed, and temperature. The data is utilized to update the actual power of DRESSs as needed, which can be calculated using equation (4).

$$P_{swt}(t) = \begin{cases} 0, & \text{if } v(t) < v_{ci} \text{ or } v(t) > v_{co} \\ \frac{v^3(t) - v_{ci}^3}{v_r^3 - v_{ci}^3}, & \text{if } v(t) > v_{ci} \text{ \& } v(t) < v_r \\ 1, & \text{if } v(t) > v_r \text{ \& } v(t) < v_{co} \end{cases} \quad (1)$$

$$T_c(t) = T_{am}(t) + I_{gs}(t) \frac{IOCT - 20}{0.8} \quad (2)$$

$$P_{spv}(t) = Y_d \frac{I_G(t)}{I_S} \left[1 - \frac{K_p}{100} (T_c(t) - T_{STC}) \right] \quad (3)$$

$$P_{drs}^{act}(t) = \beta_{swt} \cdot (1 - D_{swt})^{plt} \cdot P_{swt}(t) + \beta_{spv} \cdot (1 - D_{spv})^{plt} \cdot P_{spv}(t) \quad (4)$$

The cut-in, rated, and cut-out wind speeds are denoted as v_{ci} , v_r , and v_{co} , respectively. Considering the significant dependence of these parameters on the size of the SWT, a 50 kW wind turbine was selected for the design objective. The chosen values for these parameters are 3, 10, and 20 m/s for v_{ci} , v_r , and v_{co} , respectively.

2) *PEVs Charging*: When the PEV is at rest in its home location, the SOC of its battery for each time interval is expressed by equation (5). The power available for charging the PEV is calculated using equation (6).

$$SOC_{pev}(t + \Delta t) = SOC_{pev}(t) + \frac{P_{pev}^{chr}(t) \cdot \eta_{pev}^{chr} \cdot \Delta t}{E_{pev}} \quad (5)$$

$$P_{pev}^{ip}(t) = \min(\beta_{pev} \cdot P_{pev}, (E_{pev}/\Delta t)) \cdot (SOC_{pev}^{max} - SOC_{pev}(t)) \quad (6)$$

3) *Battery Charging*: During each time interval, the charging/discharging power of the Battery Storage System (BSS) must not surpass an available power limit. The input and output power limits for charging/discharging of BSS are determined by equations (7) and (8), while the SOC of BSS for each time interval is computed by equation (9).

$$P_{bss}^{ip}(t) = \min \left(\beta_{bss} \cdot P_{bss}, \left(\frac{E_{bss}^{act}}{\Delta t} \right) \times (SOC_{bss}^{max} - SOC_{bss}(t)) \right) \quad (7)$$

$$P_{bss}^{ot}(t) = \min \left(\beta_{bss} \cdot P_{bss}, \left(\frac{E_{bss}^{act}}{\Delta t} \right) \times (SOC_{bss}(t) - SOC_{bss}^{min}) \right) \quad (8)$$

$$SOC_{bss}(t + \Delta t) = SOC_{bss}(t) + \frac{(P_{bss}^{chr}(t) \cdot \eta_{bss}^{chr} - P_{bss}^{dch}(t) / \eta_{bss}^{dch}) \cdot \Delta t}{E_{bss}^{act}} \quad (9)$$

$$E_{bss}^{act} = \beta_{bss} \cdot E_{bss} \quad (10)$$

Where η_{bss} is the efficiency of BSS. Δt is the time interval.

4) *Inverter*: The inverter's nominal capacity ought to exceed the power that flows through it.

$$\eta_{inv} \cdot (P_{drs}^{act}(t) + P_{bss}^{dch}(t)) \leq \beta_{inv} \cdot P_{inv} \quad (11)$$

Where as η_{inv} efficiency of inverters.

III. OPTIMAL CAPACITY PLANNING MODEL

In this section, the objective function for sizing is described, constraints are discussed, and the problem-solving process involves utilizing a semi-supervised machine learning algorithm.

A. Capacity Planning and Constraints Model

The aim of this study is to minimize the cost of electricity (COE). The objective function (13) provided below represents a crucial economic metric.

$$COE = \frac{TPC + GC}{E_{hmpew}} + \frac{AC}{E_{hmpew}} \quad (12)$$

$$Objective fn = \min(COE) \quad (13)$$

Subject to the following constraints:

$$\beta_j^{\min} \leq \beta_j \leq \beta_j^{\max} \quad (14)$$

$$P_{drs}^{act}(t) + P_{imp}(t) + P_{bss}^{dch}(t) - P_{exp}(t) - P_{bss}^{chr}(t) - P_{pev}^{chr}(t) \\ = P_{hm}(t) + P_{dpd}(t) \quad (15)$$

$$SOC_{bss}^{\min} \leq SOC_{bss}(t) \leq SOC_{bss}^{\max} \quad (16)$$

$$SOC_{pev}^{\min} \leq SOC_{pev}(t) \leq SOC_{pev}^{\max} \quad (17)$$

$$0 \leq P_{bss}^{chr}(t) \leq P_{bss}^{ip}(t) \quad (18)$$

$$0 \leq P_{bss}^{dch}(t) \leq P_{bss}^{ot}(t) \quad (19)$$

$$0 \leq P_{pev}^{chr}(t) \leq P_{pev}^{ip}(t) \quad (20)$$

$$0 \leq P_{imp}(t) \leq P_{imp}^{\max} \quad (21)$$

$$0 \leq P_{exp}(t) \leq P_{exp}^{\max} \quad (22)$$

$$SOC_{pev}(\text{departure time}) \geq SOC_{pev}^{\max} \quad (23)$$

The number of components is limited, as stated in (14). Power balance, crucial for maintaining equilibrium between generation and consumption, is governed by (15). Constraints (16) and (17) set limits on the SOC for the battery and PEV, respectively. Furthermore, (18) and (19) specify the constraints on charging and discharging power for the BSS. The charging power of the PEV should not surpass the available input power, as stated in (20). The imported and exported power to/from the grid must not surpass their respective maximum values, as specified by equations (21) and (22), respectively. Lastly, (23) ensures that the SOC of the PEV at departure time remains above the specified minimum limit, as detailed in [1].

B. SSML Algorithm Model

In supervised learning, every data point is linked to an output label. This approach is also referred to as group method data handling. The algorithm gains knowledge from a labeled dataset in which input features are matched with their corresponding output labels. And in unsupervised learning, there are no predefined output labels for each data point. Instead, the algorithm explores data patterns and structures without explicit guidance, commonly tackling tasks like clustering and anomaly detection. Consider a situation where we have a limited set of labeled data (with output labels) and a significantly larger pool of unlabeled data. In semi-supervised learning, the algorithm utilizes both labeled and unlabeled data for training. The objective remains alike to supervised learning – predicting the output variable from input features. By combining labeled and unlabeled data, the hybrid technique enhances optimization by accurately predicting COE and clustering similar configurations.

1) Training Process:

(a) Generated Featured Space:

- Using historical data from various component configurations (SPV, SWT, BSS), create a feature space.

(b) For Clustering applied Unsupervised Learning:

- Apply k-means clustering to group similar configurations, assigning cluster labels to all historical data.

(c) Collected Labeled (Clustered) Data:

- Label each configuration with the cluster to which it belongs when storing the clustered data.

(d) Train the Supervised Model:

- Apply supervised regression on labeled data to predict COE based on component configurations.

2) Process to calculate Optimal Solution::

(a) Initialization:

- Set the parameters of the algorithm, like the maximum number of iterations.

(b) Iteration for Optimization:

- start iterations (1000 iterations).
- Choose a configuration at random from each cluster or according to the cluster centroids.

(c) Prediction of Unlabeled Data:

- Employ the trained unsupervised model to assign clusters for configurations lacking explicit labels.

(d) Prediction of Supervised Model:

- Forecast the COE for each chosen configuration using the trained supervised model, regardless of labeling.

(e) Optimized Processing:

- Compare the initial optimal COE0 with the COE of the newly chosen configuration.
- Update COE0 to reflect the new COE if the current COE is lower than COE0.

(f) Track the Optimized Solution:

- Maintain a record of the ideal configuration producing the lowest COE.

(g) End Condition:

- Reached the predetermined maximum number of iterations, stop the iterations.

TABLE I
COMPARISON IN COMPUTING COE MAXIMUM CAPACITY OF
COMPONENTS AND TIME BY VARIOUS ALGORITHMS

Method	COE (\$/kWh)	SPV (kW)	SWT (kW)	BSS (kWh)	IVT (kW)	Time (sec)
SSML	25.83	19	6	2	17	5.32
GMDH [1]	26.77	20	5	2	17	5.46
MLP [9]	26.89	19	9	4	16	23.26
PSO [8]	26.84	20	6	3	17	124.21

IV. CASE STUDY

In this study, a real system from Adelaide, Australia, was examined through an actual case study, considering a three-phase grid-connected houses.

A. Technical and Economic Data

Tariffs based on TOU regulations determine electricity import and export rates. Off-peak (21–07) and peak hours (08–20) import prices are 27.90 ¢/kWh and 42.90 ¢/kWh, respectively [1]. The export rate is set at one-third of the import price. Costs are presented in Australian dollars. Project input data and component details such as PEV, solar, wind, inverter, and battery are sourced from [1]. SPV experiences a 0.95% annual degradation [5]. SWT undergoes a 1.6% annual deterioration. BSS and PEV batteries have a 92% round-trip efficiency, with a 10-year project lifespan. Grid limitations prevent overloading. Values align with current South Australian market pricing.

B. Meteorological and Load Consumption Data

Utilizing real hourly wind velocity and solar radiation data obtained from the Australian Government's Bureau of Meteorology Climate Data Online [12] the actual power generated by DRESs was calculated by equation (4), as shown in Figure 3. Load consumption data for a typical South Australian house is sourced from [1], providing average, minimum, and maximum values of 0.83 kW, 0.32 kW, and 3.41 kW, respectively. The annual energy consumption is recorded as 4136.676 kWh [5]. Annually, Australia receives over 58 million petajoules of solar radiation, exceeding the country's energy use 10,000 times. In South Australia, the average daily solar exposure is 7.12 kWh/m²/day, and the average ambient temperature is 17.9 °C [7]. A 1 kW solar system yields a daily generation of 6.12 kWh. For wind velocity, minimum, average, and maximum values are 0.00 m/s, 6.10 m/s, and 13.63 m/s, respectively.

C. Annual Stochastic Data For PEV

The lognormal probability distribution function (PDF) was employed to model the arrival SOC of PEVs and their associated data, including departure and arrival times. [1]. Annual

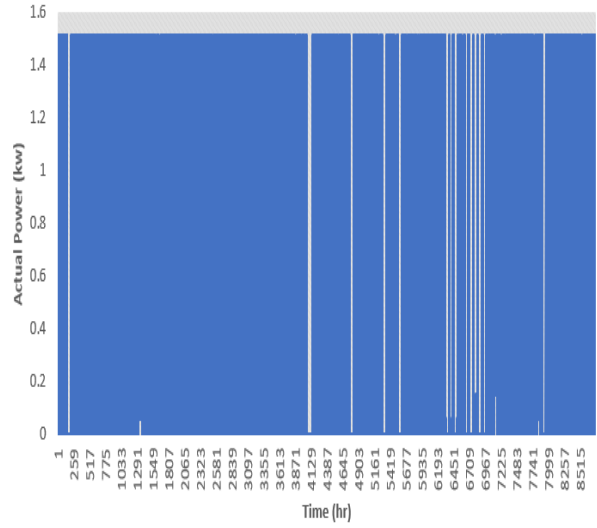


Fig. 3. Actual power of distributed energy.

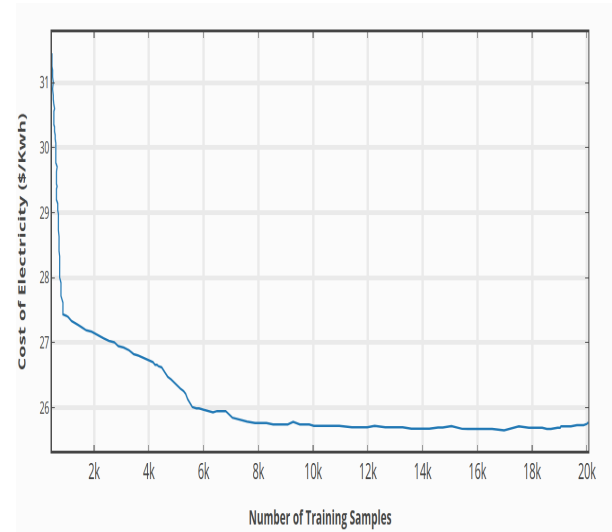


Fig. 4. The Impact of Training Sample Size for SSML on the COE.

stochastic statistics for the PEV's initial SOC upon arrival and departure/arrival times are provided [1]. In comparison, the smart slow charger, priced at \$800 for a 7 kW output, is contrasted with the smart fast charger, priced at \$1200, capable of reaching a charging power of 22 kW [2]. Both chargers have a 10-year lifespan.

V. RESULTS AND DISCUSSION

The experiments in this study were carried out on Google Colab [10], an open-source platform provided by Google. To implement the operational strategy in DRESs, the proposed model was built using Python 3.11 64-bit [11]. The proposed SSML algorithm technique is applied to a typical DRESs System model for homes connected to the grid with fast-charging PEVs. Optimization results were obtained by

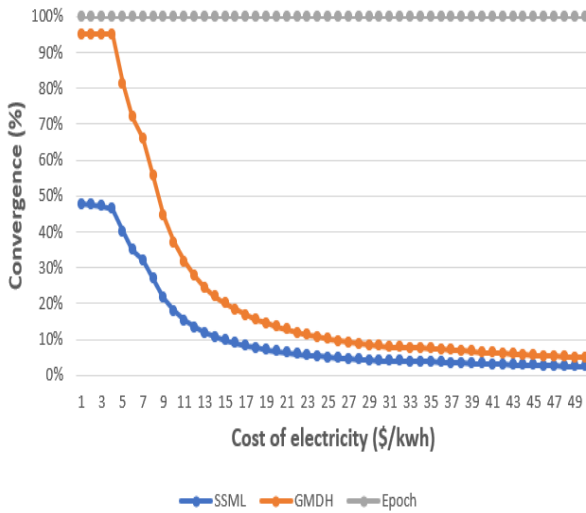


Fig. 5. Convergence pattern of SSML and GMDH.

employing various algorithms in this study, and the training process of semi-supervised learning was analyzed, along with the sizing of components.

A. Analysis of Training Process of SSML

Fig. 4 demonstrates the application of SSML algorithm in this study to achieve the lowest COE. Optimization was conducted with varying training sample sizes, ranging from 500 to 20,000 in increments of 500 samples for SSML training. Notably, the SSML algorithm consistently achieves a minimal COE of \$25.83/kWh, and this performance remains constant even beyond 9,000 samples. Therefore, 9,000 samples were considered a reliable quantity for training the SSML algorithm for optimal sizing.

B. Optimal Capacity With Different Algorithms

When compared to alternative methods, the SSML approach demonstrates the lowest COE, as depicted in Table I. Specifically, the COE is 0.94 \$/kWh lower than for GMDH approach and exhibits superior performance compared to MLP technique. In addition, when compared to multi-layer perceptron (MLP) method, the PSO algorithm demonstrates a lower COE by approximately 0.05 \$/kWh. The computational time associated with SSML is 5.32 sec and is the lowest compared to other algorithms.

C. Convergence Pattern of ML

Fig. 5 illustrates the convergence patterns for SSML (semi-supervised machine learning) and GMDH (group method data handling). Both machine learning methods run for 100% of the generation, where a generation represents how many times all training vectors are utilized to update weights in machine learning algorithms. The SSML approach converges to minimum COE at 8% of the generation, while GMDH converges at 12% of the generation for their respective COEs.

D. Advantages of SSML compared to GMDH

This paper employed unlabeled data, by handling limited labeled data, enhancing model robustness, capturing complex patterns, reducing dependence on expert labeling, adapting to changing environments, and exploring novel configurations.

VI. CONCLUSION

This study designed a model for a distributed renewable energy source system in grid-connected homes with plug-in electric vehicles using the semi-supervised machine learning algorithm. Optimal capacity results were obtained for SPV, SWT, and BSS at 19 kW, 6 kW, and 2 kW, respectively. The convergence was faster compared to existing studies, and the COE was 0.94 \$/kWh less than the existing study that uses GMDH algorithm.

This research can be further extended by incorporating different charging models, especially with DC fast charging infrastructure to reduce charging time. Additional enhancements may include exploring various machine learning algorithms and evaluating their impact on the cost of electricity for vehicle-to-grid and vehicle-to-home scenarios.

REFERENCES

- [1] R. Khezri, P. Razmi, A. Mahmoudi, A. Bidram, and M. H. Khooban, "Machine learning-based sizing of a renewable-battery system for grid-connected homes with fast-charging electric vehicle," *IEEE Transactions on Sustainable Energy*, vol. 14, no. 2, pp. 837–848, Dec. 5, 2022.
- [2] Y. Zhang, Y. Zhou, C. Jiang, Y. Wang, R. Zhang, and G. Chen, "Plug-in electric vehicle charging with multiple charging options: A systematic analysis of service providers' pricing strategies," *IEEE Trans. Smart Grid*, vol. 12, no. 1, pp. 524–537, Jan. 2021.
- [3] F. Hafiz, A. R. de Queiroz, and I. Husain, "Coordinated control of PEV and PV-based storages in residential systems under generation and load uncertainties," *IEEE Trans. Ind. Appl.*, vol. 55, no. 6, pp. 5524–5532, Nov./Dec. 2019.
- [4] R. Khezri, A. Mahmoudi, and H. Aki, "Optimal planning of solar photovoltaic and battery storage systems for grid-connected residential sector: Review, challenges and new perspectives," *Renewable and Sustainable Energy Reviews*, vol. 153, p. 111763, Jan. 1, 2022.
- [5] R. Khezri, A. Mahmoudi, and M. H. Haque, "Optimal capacity of solar PV and battery storage for Australian grid-connected households," *IEEE Trans. Ind. Appl.*, vol. 56, no. 5, pp. 5319–5329, Sept./Oct. 2020.
- [6] S. Bandyopadhyay, G. R. C. Mouli, Z. Qin, L. R. Elizondo, and P. Bauer, "Techno-economical model based optimal sizing of PV-battery systems for microgrids," *IEEE Trans. Sustain. Energy*, vol. 11, no. 3, pp. 1657–1668, Jul. 2020.
- [7] B. Mohandes, S. Acharya, M. S. E. Moursi, A. S. Al-Sumaiti, H. Doukas, and S. Sgoridis, "Optimal design of an islanded microgrid with load shifting mechanism between electrical and thermal energy storage systems," *IEEE Trans. Power Syst.*, vol. 35, no. 4, pp. 2642–2657, Jul. 2020.
- [8] S. Kahrobaee, S. Asgarpoor, and W. Qiao, "Optimum sizing of distributed generation and storage capacity in smart households," *IEEE Trans. Smart Grid*, vol. 4, no. 4, pp. 1791–1801, Dec. 2013.
- [9] H. Ren, Z. Ma, W. Lin, S. Wang, and W. Li, "Optimal design and size of a desiccant cooling system with onsite energy generation and thermal storage using a multilayer perceptron neural network and a genetic algorithm," *Energy Convers. Manage.*, vol. 180, pp. 598–608, 2019.
- [10] Google Colaboratory. Accessed: [3/07/2023]. [Online]. Available: <https://colab.research.google.com/>
- [11] Python Software Foundation. Python 3.11.0 Documentation. Accessed: [18/05/2023]. [Online]. Available: <https://docs.python.org/3.11/>
- [12] Australian Government, Bureau of Meteorology. Climate Data Online, Accessed: Sep. 2021. [Online]. Available: <http://www.bom.gov.au/climate/data/index.shtml?bookmark=200>